Polish Journal of Chemical Technology, 20, 1, 35—46, 10.2478/pjct-2018-0006

Energy efficiency analysis of styrene production by adiabatic ethylbenzene dehydrogenation using exergy analysis and heat integration

Emad Ali, Mohamed Hadj-Kali

King Saud University, Chemical Engineering Department, Riyadh, Saudi Arabia 11421
**Corresponding author: e-mail: amkamal@ksu.edu.sa*

Styrene is a valuable commodity for polymer industries. The main route for producing styrene by dehydrogenation of ethylbenzene consumes a substantial amount of energy because of the use of high-temperature steam. In this work, the process energy requirements and recovery are studied using Exergy analysis and Heat Integration (HI) based on Pinch design method. The amount of steam plays a key role in the trade-off between Styrene yield and energy savings. Therefore, optimizing the operating conditions for energy reduction is infeasible. Heat integration indicated an insignificant reduction in the net energy demand and exergy losses, but 24% and 34% saving in external heating and cooling duties, respectively. When the required steam is generated by recovering the heat of the hot reactor effluent, a considerable saving in the net energy demand, as well as the heating and cooling utilities, can be achieved. Moreover, around 68% reduction in the exergy destruction is observed.

Keywords: Styrene production, Ethylbenzene dehydrogenation, Exergy analysis, Heat Integration, Pinch Analysis, Heat Recovery.

INTRODUCTION

Styrene (ST) is the second principal monomers in the chemical industries because it is a key raw material of polymers. It is used to produce versatile polymeric materials, the main products being poly-styrene, styrene-acrylonitrile, styrene-butadiene latex and acrylonitrile-butadiene styrene resins (ABS)[1]. The utilization of styrene-based plastics is growing quickly. Currently, polystyrene is the least expensive thermoplastics in terms of a cost-per-volume basis[2]. The major commercial process to produce styrene is the dehydrogenation of ethylbenzene (EB), in which adiabatic dehydrogenation accounts to 90% of the commercial production[1, 3]. In 2010 the total annual production of styrene reached 26.4 million metric tons[4]. The expected worldwide consumption of styrene in 2020 is expected to increase to 41 million metric tons[5].

Sufficient work on kinetics and reactor modeling for Styrene production by dehydrogenation of ethylbenzene is available in the literature. Snyder and Subramniam[6] developed a heterogeneous model to investigate the effect of using a novel, packed-bed, reverse flow reactor for the endothermic dehydrogenation of ethylbenzene to styrene. They showed that dividing the steam injection over various locations gives *near isothermal* bed temperatures. Desirable overall ethylbenzene conversion and styrene selectivity are obtained due to isothermal operation. Similarly, Haynes et al.[7] extended the concept of the reverse flow reactor to endothermic reactions such as dehydrogenation of ethylbenzene. They showed that higher conversions than conventional systems can be achieved by the periodic alternation of a reactant and a regenerating medium counter currently over a fixed bed of catalyst. Abdalla et al.[8] developed kinetics model of an industrial catalyst for the dehydrogenation of ethylbenzene to styrene. The rigorous heterogeneous model is validated using industrial reactor data based on the Stefan-Maxwell equations for multicomponent diffusion in porous catalyst pellets. Hossain et al.[9] proposed another phenomenological-based kinetics model for the dehydrogenation of ethylbenzene to styrene over a FeOx-meso-Al_2O_3 catalyst based on a joint surface science and engineering approach. Tamsilian[10] presented a mathematical model for ethylbenzene dehydrogenation consists of nonlinear simultaneous differential equations with multiple dependent variables. They concluded that application of the proposed catalyst increases ethylbenzene conversion and decreases necessary inlet temperature. Zarubina[11] screened high throughput catalyst involving catalysts based on bare commercial carriers, metal-based counterparts, carbon-based materials, and P-promoted catalysts. The purpose was to achieve conversion higher than the conventional one. Lee[12] developed a mathematical model for the ethylbenzene dehydrogenation based on validated kinetics model using experimental data. The comprehensive model is used to estimate the steam to ethylbenzene ratio that leads to optimum operating conditions.

The current conventional styrene production by steam dehydrogenation suffers from several disadvantages: (1) High energy consumption due to the use of superheated steam, (2) The reaction is thermodynamically limited to 50–65%, which demands a considerable reactant recycle, (3) Separation of EB and ST is problematic due to a similar boiling point of 136°C and 145°C, respectively[11, 13–16]. Alternately, the oxidative dehydrogenation of ethylbenzene (EB) has been proposed to overcome equilibrium limitation regarding conversion when operating at lower temperatures with an exothermic reaction[17]. However, this process suffers from loss of styrene selectivity due to the production of carbon oxides and oxygenates[14]. In addition, the use of oxidant compromises the process safety as it should always operate outside of the flammability limits of ethylbenzene[11]. Isothermal dehydrogenation of ethylbenzene to styrene is also studied. However, this approach is not widely spread and has limited production capacity[10].

To alleviate the energy consumption due to the use of steam, efforts to replace the steam with CO_2 are studied. It is believed that utilization of CO_2 instead of steam will have beneficial advantages such as energy saving

by avoiding high loss of water latent heat, and lower reaction temperature due to the ability to overcome the thermodynamic equilibrium. Mimura et al.[18] pointed that the energy required for the CO_2-based process for the dehydrogenation of ethylbenzene to produce styrene was found to be substantially less than that of the steam--based commercial process because CO_2 remain gaseous throughout the process. Mimura and Saito[15, 16] studied the relationship between the yield of styrene and the energy required for separation by distillation when CO_2 is used for styrene production from ethylbenzene. Park and Chang[14], demonstrated the use of CO_2 as an oxidant in the dehydrogenation of ethylbenzene to styrene to reduce energy consumption and overcome equilibrium limitation. However, no process for styrene production using CO_2 has been commercialized to date.

To increase ethylbenzene conversion beyond the thermodynamic equilibrium several authors have suggested the use of selective membranes to remove hydrogen from the reaction mixture and hence to suppress the reverse reaction. Abdalla & Elnashaie[19], investigated the use of a rigorous heterogeneous model to study the effect of using selective membranes over porous support materials for the removal of hydrogen on the conversion of ethylbenzene to styrene by dehydrogenation. Similarly, Hermann et al.[3] showed that the kinetic limitation can be overcome and ethylbenzene conversion can be increased to above 90% without compromising styrene selectivity. This can be obtained by increasing the reactor pressure in the membrane reactor. Vaezi et al.[20] studied the catalytic dehydrogenation of ethylbenzene to styrene in a simulated tubular membrane reactor. It is reported that Ethylbenzene conversion and styrene yield can be increased to 3.45% and 8.99%, respectively which is attributed to the effect of hydrogen removal from reaction side. In the same line, Akpa et al.[1] developed first-principles models to estimate the ethylbenzene conversion and the product's selectivity in a catalytic membrane reactor for the dehydrogenation of ethylbenzene. The adequacy of the resulted models was verified against industrial plant data. The models were afterward used to study the impact of the reactor inlet conditions.

Clearly, the main challenge of the traditional styrene process lies in the economic production. Most of the alternative technologies discussed earlier either not yet commercialized and/or suffer from other shortcomings. Bearing in mind that styrene demand is increasing (Nederlof, 2012), small enhancements in the efficiency of the existing plant operation can generate a large profit. Therefore, it might be worthwhile to enhance the present technology by maximizing the steam utilization while optimizing styrene selectivity and/or retrofit the heat recovery system for the existing plant. Therefore, the objective here is to seek energy-efficient configuration of the current styrene process by utilizing heat integration and judicious exergy analysis. Heat integration is widely used in many industrial sectors such as, but not limited to, oil & gas, chemical & petrochemical, pulp & paper, metal production, dairies, breweries, and pharmaceuticals[21]. Specifically, Yoon et al.[22] studied retrofitting Ethylbenzene production by alkylation of Benzene and Ethylene using Pinch analysis. The proposed Heat Exchanger Network can reduce the annual energy cost by 5.6%. The attempt to reduce the energy consumption of the existing Styrene plant will cause relevant countless returns and achieve sustainable development against circumstantial challenges.

PROCESS DESCRIPTION

Styrene is produced traditionally by catalytic dehydrogenation of ethylbenzene. The chemical reaction is highly endothermic carried out in the vapor phase at a temperature ranging between 500 and 700°C[11]. An excess of superheated steam of 720°C is added to the reactant mixture with steam/EB molar ratios of 6–13:1[11] with higher values such as 15:1 to 20:1 are also reported[23, 24]. Steam provides the required heat of reaction, avoids excessive coking or carbon deposition, shifts the equilibrium of the reversible reaction toward the selected products, and scrubs the catalyst from any existing carbon. Benzene (B), toluene (T), methane, and ethylene (E) are the main byproducts. Because the reaction is endothermic and reversible, it involves the evolution of a number of gaseous moles. Thus, high conversion necessitates elevated temperatures and a low EB partial pressure[25].

The typical flow sheet for production of Styrene from Ethylbenzene by adiabatic dehydrogenation is shown in Figure 1, which represents typical commercial plants[26]. The flow sheet contains the operating temperature and pressure as well as the vapor fraction of each stream as taken from open literature[27]. These operating conditions will be considered fixed as the baseline conditions. Normally, the solution of the mass balance equations will not be affected by these operating conditions unless the resulted mole fraction does not reproduce the nominal vapor fraction at the given pressure and temperature. In this case, vapor-liquid equilibrium model will be solved to find the new stream's temperature that makes the corresponding vapor fraction matches the nominal baseline. Combined fresh and recycled Ethylbenzene is fed to the adiabatic reactor after mixing with high-temperature steam at a specific ratio. The steam raises the feed temperature to the required reaction temperature and provides the necessary energy for the endothermic reactions. EB conversion to Styrene takes place in two reactors in series (R-101 and R-102). The resulted gases are cooled and then separated in three separation columns in series to produce fresh Styrene. The light gases such as hydrogen, methane, and ethylene are separated from the rest of components in a three-phase separator (S-101). Liquid water is also extracted in this column. The remaining hydrocarbon components are separated in the subsequent distillation columns based on their corresponding boiling point. Saturated steam at 42.4 bar is super-heated to desired temperature in a fired--heater (F101) before being fed to the reactor. The saturated steam is usually supplied from a steam turbine. However, for carrying the exergy and heat integration, we introduced a typical heat exchanger to generate the saturated steam The Chemical reactions that take place in the reactors are given as follows[6, 10]:

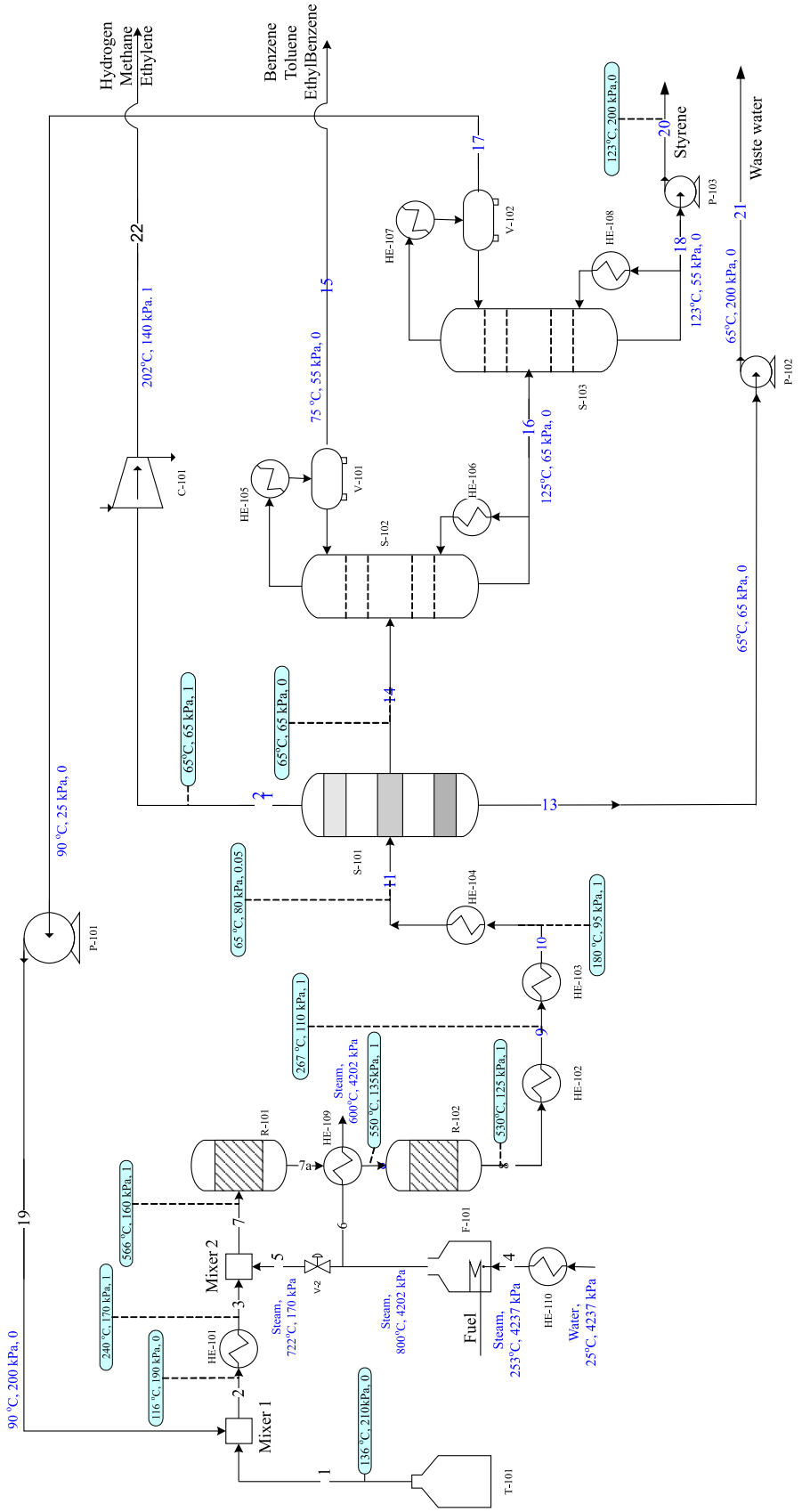

Figure 1. Styrene Production flow sheet

$$C_6H_5C_2H_5 \overset{r_1,r_{1r}}{\longleftrightarrow} C_6H_5C_2H_3 + H_2$$

$$C_6H_5C_2H_5 \overset{r_2}{\rightarrow} C_6H_6 + C_2H_4$$

$$C_6H_5C_2H_5 + H_2 \overset{k_3}{\rightarrow} C_6H_5CH_3 + CH_4$$

With the kinetics of the reactions are given a s follows[6, 10]:

$$r_1 = 1.177 \times 10^8 \exp\left(-\frac{21708}{RT}\right) p_{eb} \quad (1)$$

$$r_{1r} = 20.965 \exp\left(\frac{7804}{RT}\right) p_{sty} p_{hyd} \quad (2)$$

$$r_2 = 7.206 \times 10^{11} \exp\left(-\frac{49675}{RT}\right) p_{eb} \quad (3)$$

$$r_3 = 1.724 \times 10^6 \exp\left(-\frac{21857}{RT}\right) p_{eb} p_{hyd} \quad (4)$$

Where T in Kelvin, R=1.987 cal/mol · K, and r_i in mol/m^3 · s Note that the first reaction is limited by thermodynamic equilibrium which is given as[10]:

$$K = \frac{y_{sty} y_{hyd} P}{y_{eb}} \quad (5)$$

and

$$\ln K = 15.5408 - \frac{148526}{T} \quad (6)$$

Where T in Kelvin and P in *bar*. Therefore, r_1 and r_{1r} can be combined as follows:

$$r_1 = 1.177 \times 10^8 \exp\left(-\frac{21708}{RT}\right)\left(p_{eb} - \frac{p_{sty} p_{hyd}}{K}\right) \quad (7)$$

NUMERICAL SOLUTION METHODOLOGY

To determine the mass/mole rate for each stream in the flow sheet, the mass balance equation for the entire process must be solved for given constraints. This step requires fixing the degrees of freedom of the process flow sheet. The process has 38 unknowns comprises all component's molar rate in the entire process. In addition, the extent of the chemical reactions presents additional 3 unknowns to make the total unknown variables equal 41. On the other hand, 34 relations are available which comprises 31 mass balance equations plus 3 given reaction kinetics. Therefore, additional 7 relations are required to make the degrees of freedom equal zero and to exactly solve the design equations. For this purpose, 7 numerical constraints are selected for key variables as listed in Table 1. The EB feed rate and other specifications are chosen such that it corresponds to Styrene production of 100k tons per year[12]. These specifications are taken from the literature[27] to formulate the baseline for all calculations. The procedure for solving the design equations and exergy are explained by the algorithm shown in Figure 2. Given the operating conditions (T, P, V_L) and the design specifications in Table 1, the mass balance equations and reactor model are solved simultaneously to determine the composition and flow rate for all streams. The phase condition of each stream is checked against the pre-defined one. If it does not match, the temperature is re-calculated such that the phase conditions are satisfied. Afterward, the flow rate of the auxiliary streams used in the heat exchangers is computed using energy balance. The inlet and outlet temperature of each auxiliary stream are pre-specified as given in the literature[27]. Note that these temperatures are considered always fixed. If the

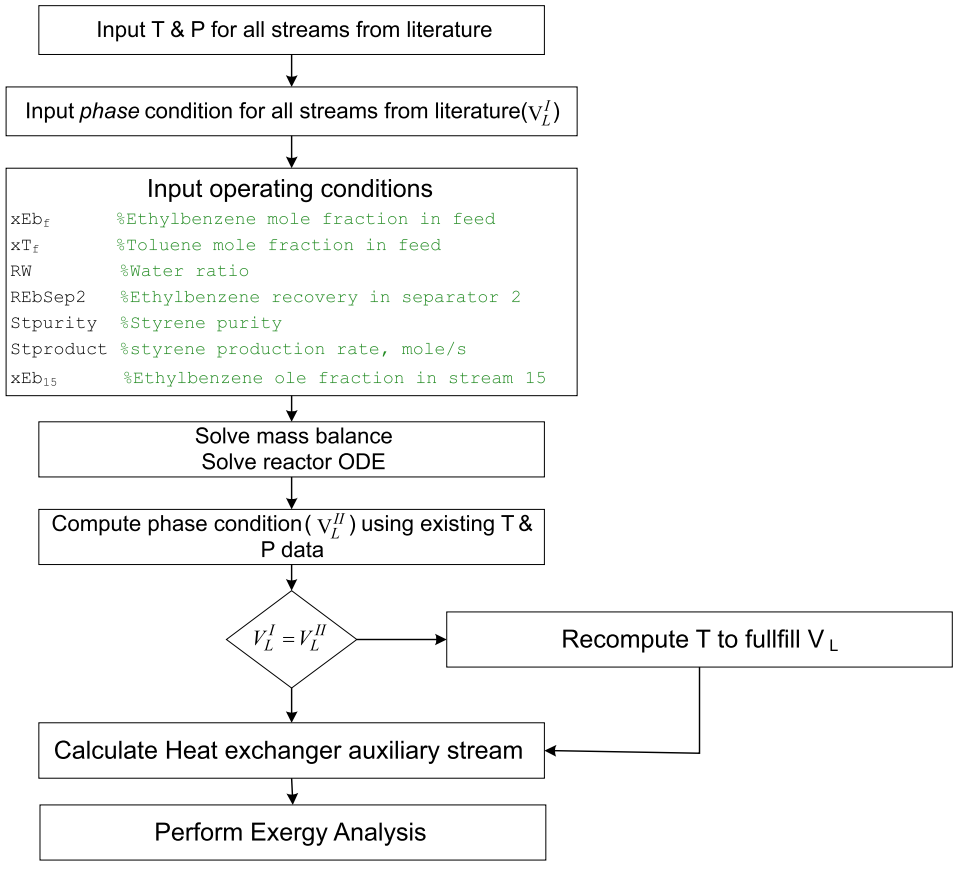

Figure 2. Method of solution

Table 1. List of design constraints & KPI

Design parameters	Arbitrary[27]	KPI	Maximum yield
Ethylbenzene feed rate [kmol/h]	120.81	Eb conversion [%]	53.43
Mole Fraction of Ethylbenzene in Feed	0.98	Styrene selectivity [%]	99.43
Mole fraction of Toluene and Benzene	0.1	Toluene selectivity [%]	0.45
Purity of ST product	0.9996	Benzene Selectivity [%]	0.12
Mole fraction of Ethylbenzene in stream 15	0.03	Exergy destruction [MW]	37.16
% EB Recovery in Separator 2	99.90	Total energy [MW]	29.75
Steam ratio	13.26	Specific energy [MJ/kg Styrene]	8.58
		Exergy Efficiency [%]	35.51
		Yield [mole St/mole Eb]	0.993

heat exchanger conditions changed, only the flow rate is re-computed to meet the energy balance constraints. Exception is for HE-109 where the steam flow rate is fixed while its outlet temperature can be altered to meet any perturbation in the heat exchanger balance. When the flow rate, vapor fraction, temperature, and pressure are determined for all streams, the exergy balance will be carried out. In addition, the energy load for every heat exchanger using external energy as well as compressors and pumps will be calculated.

Solving the mass balance equation requires solving the reactor model. The reactor model is assumed as plug flow reactor and its design equations are formulated as follows[10]:

$$\frac{d}{dV}(n_{s0} + n_{eb0}X_1) = r_1 \quad X_1(0) = 0 \tag{8}$$

$$\frac{d}{dV}(n_{B0} + n_{eb0}X_2) = r_2 \quad X_2(0) = 0 \tag{9}$$

$$\frac{d}{dV}(n_{T0} + n_{eb0}X_3) = r_3 \quad X_3(0) = 0 \tag{10}$$

$$n_0 Cp\frac{dT}{dV} + CpT_0(r_1 + r_2) = \Sigma r_i \Delta H_{r_i} \quad T(0) = T_0 \tag{11}$$

Note that the subscript "0" denotes the feed conditions. Given the reactor feed condition, the ODE (Eq. 8–11) can be solved numerically over the reactor volume which is specified as 25 m^3 (for each reactor) to obtain the exit temperature and conversion (X_i) for each reaction. Therefore, the molar rate of each component exiting the reactor can be found from:

$$n_{eb} = n_{eb0}(1 - X_1 - X_2 - X_3) \tag{12}$$

$$n_S = n_{S0} + n_{eb0}X_1 \tag{13}$$

$$n_H = n_{eb0}(X_1 - X_3) \tag{14}$$

$$n_T = n_{T0} + n_{eb0}X_3 \tag{15}$$

$$n_B = n_{B0} + n_{eb0}X_2 \tag{16}$$

$$n_E = n_{eb0}X_2 \tag{17}$$

$$n_M = n_{eb0}X_3 \tag{18}$$

The pressure of the gases exiting the reactor can be found from:

$$P = \frac{n_t RT}{v} \tag{19}$$

Where n_t is the total outlet molar rate and the overall volumetric flow rate, v is calculated by:

$$v = v_0(1 + \zeta_1 X_1 + \zeta_2 X_2 + \zeta_3 X_3) \tag{20}$$

Where ζ_i is the extent of each reaction whereas the inlet volumetric flow rate, v_0 is computed from the ideal gas law as follows:

$$v_o = \frac{n_o RT_0}{P_0} \tag{21}$$

The reactor ODE model is solved numerically using Euler method. To guarantee accuracy and stability of Euler method a step size of 0.1 is used. The reaction rates are given in Eq. 1–4 are a function of the component's partial pressure, therefore, they can be reformulated in terms of reaction conversion by expressing the partial pressure as follows:

$$p_i = \frac{n_i}{n_t} P \tag{22}$$

It should be noted that developing a rigorous model is not of interest here. The purpose is to use a reasonable model to carry out the energy analysis. The solution algorithm shown in Figure 2 involves estimation of the phase condition. The phase condition is determined by the following algorithm[28]:

Case 1: if $T > T_{cj}$ for all components, then $V_L = 1$

Case 2: if $T < T_{cj}$ for all components, then check T_{dp} and T_{bp} for the mixture:
If $T > T_{dp}$, then $V_L = 1$
If $T < T_{bp}$, then $V_L = 0$
If $T_{bp} \leq T \leq T_{dp}$, then check VLE using flash calculations.

Case 3: If $T > T_{cj}$ from some components and $T < T_{cj}$ for others, then check T_{dp}:
If $T > T_{dp}$, then $V_L = 1$
If $T < T_{dp}$, then check VLE using flash calculations

It should be noted that dew point, bubble point, and flash calculations can be carried out using typically Raoult's law and Antione equations for vapor pressure estimation.

EXERGY PRINCIPLES

Exergy is a scientific tool helpful for sustainable design and development. It is driven from the second law of thermodynamic principles. Exergy balance of a system can provide valuable knowledge on its effectiveness. This knowledge can identify regions in which technical and other improvements should be sought. Determination of exergy losses and its sources can supply profound perception of the process performance analysis. Such analysis enables locating the component with extreme exergy destruction. Thus, improving these components lead to efficiency enhancement and optimization. Currently, exergy analysis became an engineering device for decisions making towards sustainable development[29, 30]. Indeed, Exergy is a powerful tool to assess the energy efficacy for different configurations of an existing process.

Exergy is defined as the available work that can be obtained from a fluid when it is in steady state with its surrounding environment. It is computed mathematically from[29, 30]:

$$E = (H - H_o) - T_o(S - S_o) \tag{23}$$

H_0 and S_0 represent the enthalpy and entropy values at the reference temperature T_0, which is usually equal to 298 K. H and S represent the enthalpy and entropy at a specified temperature, T (K).

In general, chemical processes transform energy and exploit exergy, hence high efficiency is of important potential. This inquires well utilization of exergy the application of effective tools. Unlike energy which is always balanced, exergy is never balanced for real processes because of irreversibilities, i.e. exergy destruction. The exergy destruction, ΔE, presents available work that can be further utilized for feasible process advancements. In Engineering applications, the exergy flows through a process can be represented by several flow diagrams, from which the scenario with the least exergy destruction can be chosen.

The exergy destruction or loss is generally expressed mathematically as follows:

$$\Delta E = \sum_{i=1}^{n} m_i E_i - \sum_{o=1}^{k} m_o E_o - Q\left(1 - \frac{T_o}{T}\right) - W \tag{24}$$

m_i and m_o denote the input and output mass flow of the system, Q is heat inflow to the system, E_i and E_o represent the specific Exergy for input and output streams respectively, and W work done on the system. *n* is the number of input streams and *k* is the number of output streams.

For adiabatic system (Q = 0) and where no work is involved (W = 0), then Eq. (24) becomes:

$$\Delta E = \sum_{i=1}^{n} m_i E_i - \sum_{o=1}^{k} m_o E_o \quad (25)$$

Martinaitis et al.[31] pointed that selection of the reference temperature plays a key role in exergy analysis. Indeed, the reference state in this paper is considered as T_0 = 298 K; P_0 = 25 *kPa*. Such conditions should simulate the ambient conditions. Exception is for the reference pressure where it selected to be the lowest value in the process flow sheet. Exergy effectiveness can be better measured and compared by exergy efficiency. Usually, the *universal* exergy efficiency is defined as[31]:

$$\eta = \frac{E_{out}}{E_{inp}} = \frac{\sum m_o E_o}{\sum m_i E_i} \quad (26)$$

RESULTS AND DISCUSSION

Optimizing the Operating Conditions

The process design parameters given in Table 1 are chosen arbitrary. Hence, it could be beneficial to look for optimal operating conditions for the plant. For this reason, the process operating conditions can be optimized to capitalize specific objective function such as styrene yield, energy requirement or specific energy requirements. The optimization problem can be formulated mathematically as follows:

$$\max_u \varphi(u) \quad (27)$$

Subject to

$$0 < u < \infty \quad (28)$$

$$f_i(u, x) = 0; \qquad i = 1, \cdots, 38 \quad (29)$$

The objective function, φ can be the styrene yield, or the total energy consumption or the specific energy requirement. When the objective function represents energy, φ will be given a negative sign to transform the optimization problem into minimization instead of maximization. *u* is the design parameters which represent the design variables listed in Table 1. Note that the first three variables, i.e. the Eb feed molar rate, Eb molar fraction in the feed and the mole fraction of Benzene in the feed are kept constant because they are the given feed conditions. The lower bound on the design parameters must be zero to avoid negative values. Note the optimization problem is constrained by the physical bounds imposed by the mass balance equations. This constraint is represented by the function *f* in Eq (29). The optimization problem is solved numerically using MATLAB software. Sequential solution method is used, i.e. in each optimization iteration, the mass balance equations and the reactor model are solved iteratively till the limits (Eq. 29) are satisfied. It turns out that the optimum operating condition that maximize the styrene yield does not differ significantly than the arbitrary conditions given in Table 1. The obtained key performance index (KPI) for the process at the optimal conditions is also listed in Table 1. The resulted KPI will be discussed later. On the other hand, when the optimization problem is carried out to minimize the total energy or specific energy consumption lead to undesirable Styrene yield. Figure 3 demonstrates how minimization of energy consumption cause unfavorable operating conditions in terms of Styrene yield. The figure shows the variation of process KPI with steam to Eb molar ratio. The molar ratio is chosen for the sensitivity analysis because it is the most effective parameter among the rest listed in Table 1. As the molar ratio increases, the reactor feed temperature increases accordingly leading to higher reaction conversion. The selectivity will improve marginally because it is already reached a thermodynamic equilibrium. Furthermore, the energy requirement will also increase due to the amplified steam consumption. Therefore, this trend is not favorable economically. On the other hand, decreasing the molar ratio will reduce the energy consumption considerably due to less steam requirements but a sharp drop in the reaction conversion and styrene yield will be obtained. Hence this direction is also undesirable. It is clear in Figure 3 that the net energy demand drops sharply at low steam ratio levels and smoothly at higher ratios. At low steam ratio levels, the energy demand declines abruptly due to two factors; the reduction in steam amount and increased cooling demand in HE105. The latter is enlarged because of the growth of Eb in the purge (stream 15) and recycle due to reduction in the reaction conversion. At high steam ratio levels, the net energy demand inclines sluggishly because of the combined surge of the heating duty of HE110 and cooling duty of HE104. In fact, the process performance is overlapping as increasing Steam to Eb ratio improves styrene selectivity but increases the separation and utility costs. Moreover, rising reaction temperature by the additional steam favors equilibrium conversion towards styrene but in the same time the side reactions become significant. As a conclusion, the arbitrary conditions for the process design variables shown in Table 1 will be considered as the optimal operating condition for yield maximization and will be used as the baseline for further process reconfiguration to enhance the energy demand and exergy efficiency which is the main goal of this work.

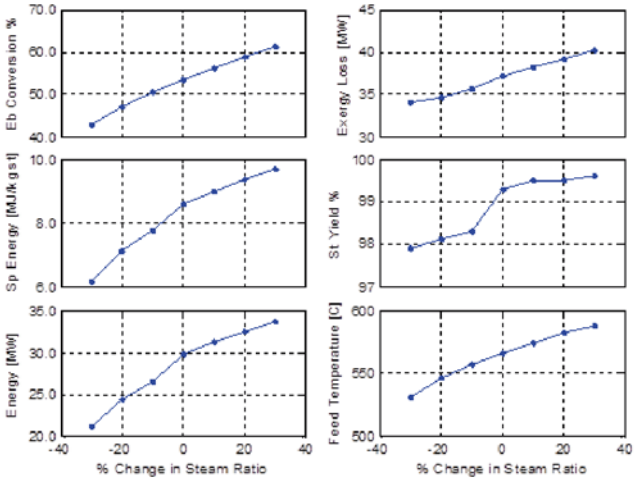

Figure 3. Process operation sensitivity against variation in the steam to Eb molar ratio

Table 2. Summary of Mass Balance

Stream No	Total Flow [kmol/h]	Temperture [K]	Pressure [kPa]	Vapor mole fraction	Water	Ethylbenzene	Styrene	Hydrogen	Benzene	Toluene	Ethylene	Methane
1	123.28	136	210	0	0	120.81	0	0	1.23	1.23	0	0
2	237.89	116	190	0	0	225.82	8.76	0	1.23	1.23	0	0
3	237.89	240	170	1	0	225.82	8.76	0	1.23	1.23	0	0
4	4031.55	253	4237	1	4028	0	0	0	0	0	0	0
5	3020.45	722	170	1	3016.9	0	0	0	0	0	0	0
6	1011.1	800	4202	1	1011.1	0	0	0	0	0	0	0
7	3258.34	566	160	1	3016.9	225.82	8.76	0	1.23	1.23	0	0
7a	3350.8	504.71	135.91	1	3016.9	133.14	101.17	92.18	1.29	1.45	0.05	0.22
8	3378.45	532	126	1	3016.9	105.16	128.74	119.43	1.37	1.77	0.14	0.54
9	3378.45	267	110	1	3016.9	105.16	128.74	119.43	1.37	1.77	0.14	0.54
10	3378.45	180	95	1	3016.9	105.16	128.74	119.43	1.37	1.77	0.14	0.54
11	3378.45	65	80	0.05	3016.9	105.16	128.74	119.43	1.37	1.77	0.14	0.54
12	120.12	65	65	1	0	0	0	119.43	0	0	0.14	0.54
13	3020.45	65	65	0	3016.9	0	0	0	0	0	0	0
14	237.89	65	65	0	0	105.16	128.74	0	1.37	1.77	0	0
15	3.25	75	55	0	0	0.11	0	0	1.37	1.77	0	0
16	234.63	125	65	0	0	105.05	128.74	0	0	0	0	0
17	114.61	90	25	0	0	105.01	8.76	0	0	0	0	0
18	120.02	122	55	0	0	0.05	119.97	0	0	0	0	0
19	114.61	90	200	0	0	105.01	8.76	0	0	0	0	0
20	120.02	123	200	0	0	0.05	119.97	0	0	0	0	0
21	3020.45	65	200	0	3016.9	0	0	0	0	0	0	0
22	120.12	202	140	1	0	0	0	119.43	0	0	0.14	0.54

Mass Balance Analysis

The outcome of solving the mass balance and reactor equations at the optimal operating condition is listed in Table 2 which shows molar rate, composition, phase condition, temperature and pressure for each stream in the process flow sheet. The summary of key performance variables is listed in Table 1. According to Table 1, the single pass conversion of Ethylbenzene reaches 53.4% which is quite within the reported values. Abdalla et al.[8] reported 47% Ethylbenzene conversion, Tasmillian et al.[10] pointed that conversion percent can lie between 60 to 75%, similarly Nederlof[13] stated that when using two reactors in series, the total conversion can reach 60–65%, finally, Behr[2] indicated that Ethylbenzene conversion in catalytic dehydrogenation reactors fall in the range of 50∼70%. It should be noted that EB conversion to Styrene is limited by thermodynamic equilibrium. The maximum equilibrium conversion can range from 80% to 88% for temperature ranging from 600 to 640°C[12, 25]. Usually, the overall reaction conversion is influenced by the catalyst type, reaction temperature, and steam to EB ratio. The Styrene selectivity calculated by our simulation approaches a high value of 99.4%. Apparently, this value is comparable with those in the literature; for example, Styrene selectivity can range from 55–85% and in some cases 90–95%[11], styrene selectivity can be as high as 96%[13]; similarly, Tasmilian et al.[10] asserted that selectivity can be in the range 87∼96% when two reactors in series are used. Styrene selectivity is a crucial factor because it maximizes the styrene production over the other side products.

Energy and Exergy Analysis

As mentioned earlier, plant economics is strongly related to energy expenses. Indeed, reduction of the energy demand can be achieved through heat recovery using heat integration without altering the process performance in terms of reaction conversion, selectivity and yield. The detailed results of the energy and exergy analysis are listed in Table 3 and 4.

Table 3. Energy Requirements

Unit	Energy [MW]		
	max yield	heat integration	ideal case
C101	0.16	0.16	0.16
P101	0.001	0.001	0.001
P102	0.003	0.003	0.003
P103	0.001	0.001	0.001
F101	27.04	27.03	27.03
E101	3.76	0	0
E102	–12.91	0	0
E103	–3.97	–2.47	0
E104	–39.67	–29.27	0
E105	–4.23	–4.37	-4.370
E106	3.6	3.6	3.6
E107	–12.86	–12.85	-12.850
E108	12.64	0	0
E110	56.32	48.05	0
Heating	**103.53**	**78.85**	**30.80**
Cooling	**–73.64**	**–48.96**	**–17.22**
Net	**29.89**	**29.89**	**13.58**

The styrene production by ethylbenzene dehydrogenation is notorious for extensive energy demands[14]. Table 3 shows that the computed energy requirements amount to 29.75 MW and the specific energy consumption per kg of styrene is 8.6 MJ, which is equivalent to 20.5×10^8 cal/ton styrene. The latter is somehow higher than that reported by Mimura et al.[18] of 15×10^8 cal/ton Styrene because different operating conditions are implemented. Accordingly, the total exergy destruction in the process as given in Table 4 is estimated to be 37.2 MW which makes the process exergy efficiency as low as 35.5%.

As mentioned earlier, the process has large exergy destruction which indicates the existence of considerable amount of useful work that can properly utilized. As indicated by Table 4, most of the exergy destruction originates from the fired heater and the exergy associated with steam fed to the fired heater. Table 3 illustrates that huge amount of external energy is required especially

Table 4. Process Exergy flow

Node	Max yield		Heat integration		Ideal case	
	Dex [MW]	%Dex	DEx [MW]	% Dex	DEx [MW]	% Dex
E1	0.29	0.50	0.29	0.61	0.29	1.62
E4	0.00	0.00	0.00	0.00	0.00	0.00
C101	0.16	0.28	0.16	0.34	0.16	0.90
P101	0.001	0.002	0.001	0.002	0.001	0.006
P102	0.003	0.006	0.003	0.007	0.003	0.019
P103	0.001	0.002	0.001	0.002	0.001	0.005
F101	16.36	28.38	16.36	34.55	16.36	91.52
E101	1.64	2.85	0.00	0.00	0.00	0.00
E106	1.06	1.84	1.06	2.24	1.06	5.93
E108	3.73	6.47	0.00	0.00	0.00	0.00
E110	34.38	59.65	29.47	62.24	0.00	0.00
Ein	**57.64**	**100.00**	**47.35**	**100.00**	**17.88**	100.00
E15	0.00	0.01	0.00	0.01	0.00	0.01
E20	0.26	0.45	0.26	0.55	0.26	1.45
E21	4.50	7.81	4.50	9.50	4.50	25.17
E22	0.18	0.31	0.18	0.38	0.18	1.01
E102	5.19	9.00	0.00	0.00	0.00	0.00
E103	0.80	1.39	0.62	1.31	0.00	0.00
E104	1.49	2.59	1.90	4.01	0.00	0.00
E105	0.16	0.28	0.16	0.34	0.16	0.90
E107	0.48	0.83	0.48	1.01	0.48	2.69
E6	7.40	12.84	7.40	15.63	0.40	2.24
Eout	**20.47**	**35.51**	**15.50**	**32.75**	**5.98**	**33.47**
Dest*	**37.17**	**64.49**	**31.84**	**67.25**	**11.89**	**66.53**

*Dest is the percentage of destroyed exergy

to super heat the steam needed for the chemical reaction. Moreover, additional external energy is required to vaporize the reactor inlet stream in HE101 and to vaporize hydrocarbon mixtures in HE106 and HE108. On the other hand, there is surplus of energy is lost via cooling and condensation in HE102~HE104 especially that lost for condensing the large amount of steam. By inspecting Table 3, the total required external energy to be supplied to the system as a heating utility is 103.5 MW while the total energy produced from cooling sums to 73.7 MW. This indicates the availability of energy to be exchanged. It should be noted though, the energy demand of HE109 is not included because it is imbedded in the energy demand of F101. The reactor outlet has a hot temperature of 532°C and contains a large amount of thermal energy that can be used to heat up other parts of the system. For this purpose, we examine process modification for optimal energy saving using heat integration approach. In the following section we seek minimization of the exergy destruction though heat integration of specific heat exchangers and sensible re-utilization of the existing exergy.

Heat Integration Based on Pinch Analysis

Heat recovery in existing plants to save energy using pinch retrofit analysis is widely used in petrochemical industries. The retrofit process involves heat integration, *i.e.* to transfer heat from the process hot streams to the process cold streams to reduce the reliance on heating and cooling duties from external utilities. This retrofit help in synthesizing a cost-effective network of heat exchangers (HEN). Different approaches have been proposed for the synthesis of HENs. These methods have been studied by Shenoy[32], Linnhoff[33], Gundersen and Naess[34] and Douglas[35]. In this section, we will follow the Heat Cascade Diagram which is a graphical representation that illustrates nicely the heat flows and decompose the heat recovery region into two sub-systems based on the pinch point location. More details can be found in (El-halwagi[36], Klemes[37]).

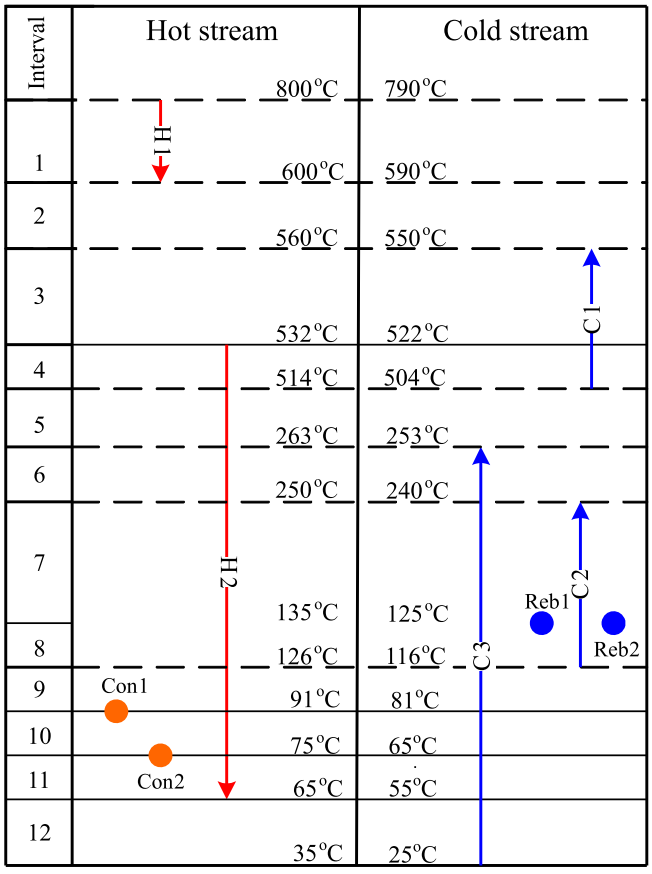

Figure 4. Temperature interval diagram

Figure 4 displays the temperature interval diagram for the hot and cold streams. H1 represent stream 6. H2 combines HE102, HE103 and HE104 for simplification. In fact, this stream takes care of cooling the second reactor effluent to the desired separator temperature. C2 represents heating the intermediate flow between reactor one and two. C1 signifies heating of stream 2 in

HE101. C3 denotes HE110 responsible for generating the high-pressure steam. In fact, the latter step requires multiple heat exchangers because it inquires large amount of energy. It is lumped in one heat exchanger for simplification. The use of heat exchanger to generate steam is customary practice in industry despite its cost and complicated design. ΔT_{min} = 10°C is used here[36]. ΔT_{min} is the minimum driving force for feasible heat transfer between the hot and cold streams such that the second law of thermodynamic is satisfied. Rigorous value for ΔT_{min} can be found by optimizing both the investment and operating costs. The corresponding cascade diagram is generated and shown in Figure 5. The cascade is developed be establishing heat balance around each interval and the surplus heat is transferred as heat residuals to the next interval with lower temperature. The tenth interval has the largest negative residual. Since negative residual is not allowed because it leads to infeasible heat exchanger design, the absolute value of the largest negative residual should be added to the top of the cascade to make all residuals non-negative. Therefore, this bottleneck locates the pinch point and the residual of 51.22 MW, which is the minimum required external heating utility. Consequently, the required external cooling utility is estimated to be 46.3 MW. Hence, the process pinch is identified to be at 116°C for cold stream and 126°C for hot stream. The next logical step is to transfer heat from the hot stream as heat source to the cold stream as heat sink as illustrated in Figure 6. Above the pinch,

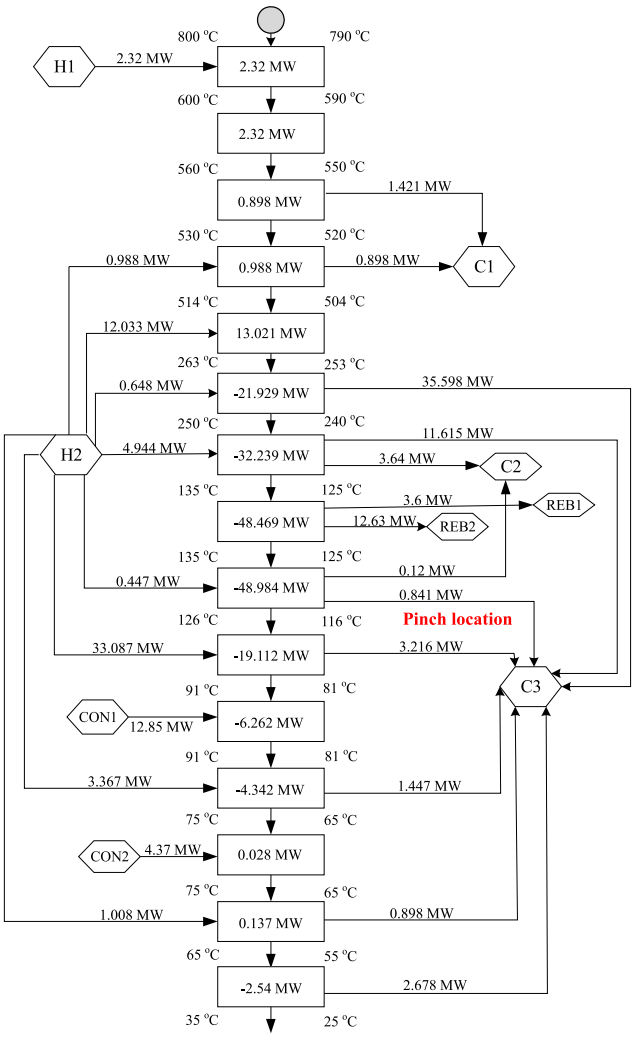

Figure 5. Heat Cascade Diagram

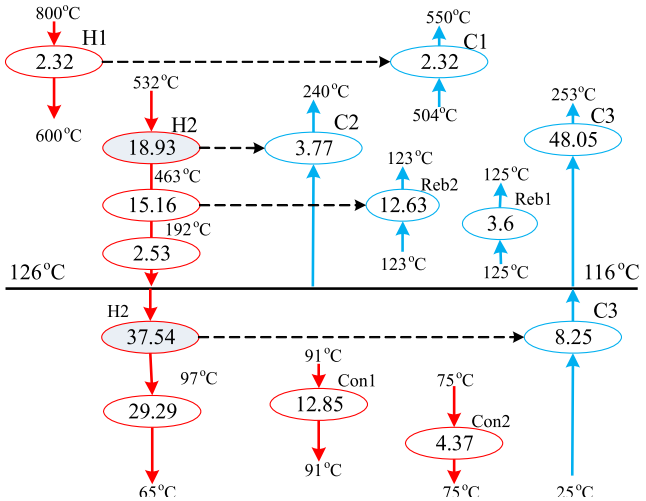

Figure 6. Stream matching above and below the pinch point

H1 and C1 is obviously matched which is the current practice in the flow sheet. Above the pinch, H1 has heat energy of 18.93 MW which is not sufficient to heat up C3 although the common practice is to match the pinch streams first. Instead, this amount of heat is recovered to provide energy to C2 and reboiler 2 (HE108). The remaining energy is 2.53 MW which is enough to supply energy for Reboiler 1 (HE106). The remaining heating requirement is 3.6 + 48.05 = 51.65 MW which is equivalent to the minimum external heating utility. Below the pinch point, the thermal energy associated with the condensers cannot be utilized to heat up C3, instead portion of H2 is transferred to C3. The remaining external cooling demand is 29.29 + 12.85 + 4.37 = 65.4 MW. The modified heat exchanger network that correspond to the matching process is shown in Figure 7. Note that Figure 7 depicts part of the overall process flow sheet to save space. In this case, the second reactor effluent exchanges its heat first with the first reactor influent, i.e. to vaporize the reactant stream. Secondly, the remaining energy is utilized to provide necessary heat for vaporization in HE108. Afterward it is cooled down in HE103 to the pinch temperature and then heat up stream 4 to the pinch temperature. Lastly, the reactor effluent must be cooled down in HE104 to the target temperature of the first separator. The effect of the proposed heat exchanger network on energy and exergy is given in Table 3 and 4. Although, the external energy requirements of some heat exchangers is either eliminated or reduce, the gross energy demand, which is defined as the difference between heating and cooling demands, remains almost the same. However, the heating and cooling duties were reduced to 79 and 49 MJ, respectively. It should be noted that HI reduces the external heating and cooling duties by the same amount via transferring energy from the hot stream to the cold stream. Therefore, the net energy requirement will remain the same. As far as exergy is concerned, small improvement in exergy destruction is obtained as the lost work is reduced from 37.16 MW to 31.84 MW. Based on the heat integration rule, heat flow across the pinch line is not allowed to avoid amplifying the external utilities usage. This limits the energy recovery scenarios. Idealistically, Figure 8, shows the heat sources and sinks above the ambient temperature without considering the pinch line. The process has two major hot streams that can provide heat energy to other

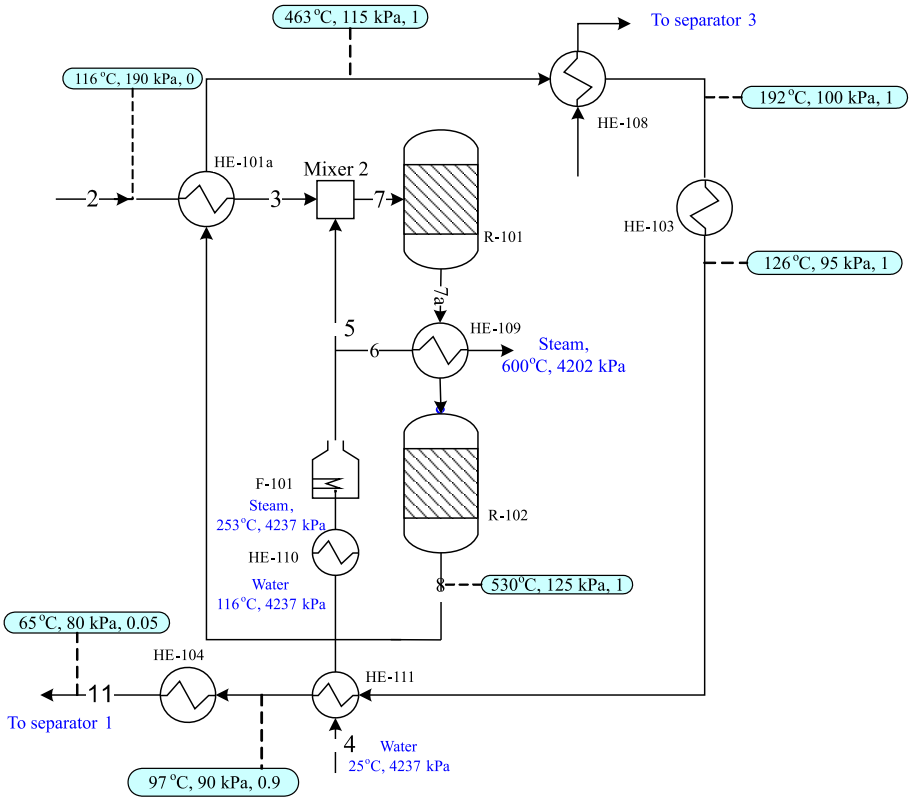

Figure 7. Heat Exchanger network based on Heat Integration

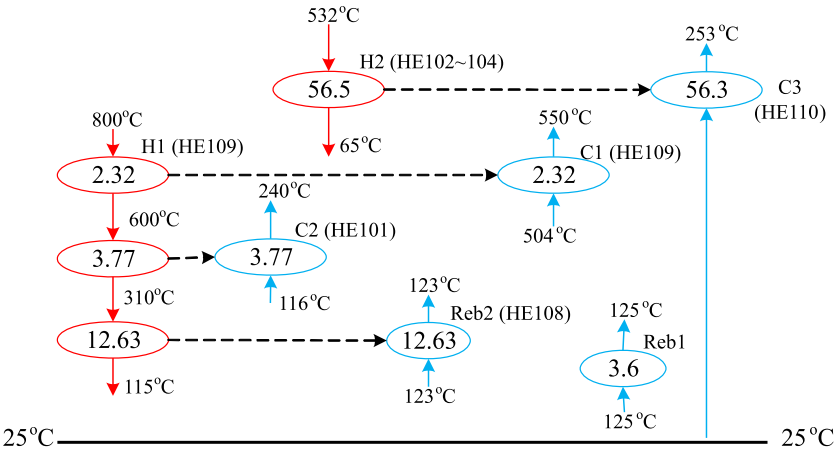

Figure 8. Energy requirement of the entire process

parts of the system which are the hot reactor effluent and the superheated steam in stream 6. On the other hand, the process has five ports where energy is required to heat up its streams. A perfect match exists between H2 and C3. Furthermore, the superheated steam is not well utilized. Heat balance calculations indicate that it is of potential to utilize the steam energy to heat up C1, C2 and HE108 sequentially. Afterward, the steam losses most of its energy and leaves HE108 as liquid at a temperature of 115°C. At this low temperature, utilizing the steam to exchange heat with HE106 is infeasible. The resulting heat exchanger layout is illustrated in Figure 9. Accordingly, the impact of the modified heat exchanger structure is apparent on the process energy and exergy characteristic as listed in Table 3 and 4. This configuration helped in reducing the net energy demand by 54%. Moreover, the destroyed exergy inside the system is minimized by 68% from 37.16 to 11.89 MW. The latter confirms as mentioned earlier the use of steam in this process is the main source of energy inefficiency. Any

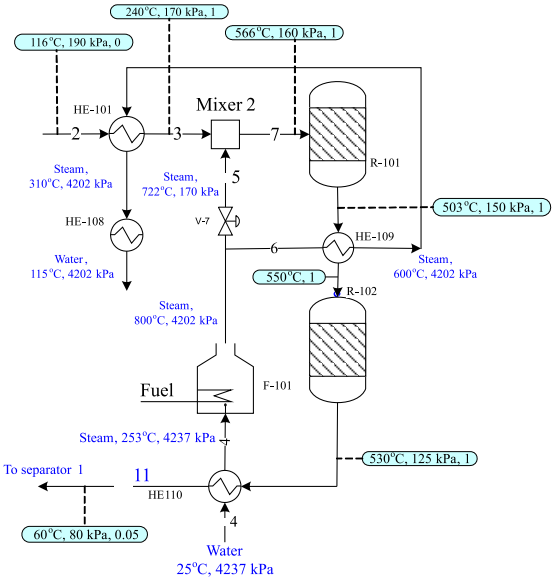

Figure 9. Heat Exchanger network based on Idealistic Heat Integration

attempt to enhance the process energy-effectiveness should tackle this issue.

CONCLUSIONS

Styrene is an important industrial commodity produced largely by adiabatic dehydrogenation of Ethylbenzene. This process is criticized for intensive energy consumption. This work aims at analyzing the energy effectiveness of the process using exergy analysis and seeks energy saving by heat integration based on pinch analysis. Simulation of the process flow sheet revealed the strong effect of the steam to Eb ratio and consequently the reactor temperature on the Styrene selectivity and production. Therefore, saving energy consumption by minimizing the steam use or its temperature may sacrifice the process performance in terms of Styrene yield. Exergy analysis indicated that the saturated steam is responsible for the largest exergy losses which amount to 60% of the total. This is because the energy produced via the steam condensation is lost without utilization. Using Pinch analysis, the minimum required external heating utility is around 52 MW mainly due to steam generation. Modification of the Heat exchanger network using heat integration approach showed insignificant improvement in the net energy demand and exergy destruction but a substantial enhancement in cooling and heating utilities. If the considerable thermal energy associated with the reactor effluent which contains a large amount of steam is recovered to generate the needed steam, remarkable saving of energy and exergy losses can be achieved.

ACKNOWLEDGEMENT

The project was supported by King Saud University, Deanship of Scientific Research, College of Engineering Research Center.

NOMENCLATURE

Cp	heat capacity, cal/moke·K
E	specific Exergy, kJ/kg
H, H_0	enthalpy and reference enthalpy, respectively, kJ/kg
K	reaction equilibrium constant
m	mass rate, kg/s
n_i	molar rate of component *i*, kmol/h
n_0	total molar rate fed for reactor 1, kmol/h
n_t	total molar rate, kmol/h
f	nonlinear function
p_i	partial pressure for component *i, bar*
P	total pressure, bar
P_0	Reactor 1 feed pressure, bar
r_i	reaction rate for reaction *i,* mol/m^3·s
R	ideal gas constant
S, S_0	Entropy and reference entropy, respectively, kJ/kg·K
T	Temperature in Kelvin
T_0	Reactor 1 feed temperature also reference temperature for exergy, K
T_{cj}	Critical temperature for component *j*, K
T_{dp}	dew point, K
T_{bp}	bubble point, K
u	design parameter
V	reactor volume, m^3
V_L	Vapor fraction
v	total volumetric flow rate, m^3/h
v_0	reactor 1 feed volumetric flow rate, m^3/h
X_i	reaction *i* conversion
x	vector of component molar rate
y_i	vapor mole fraction for component, i

Greek letter

ζ_i	stoichiometry of reaction *i*
φ	objective function
η	exergy efficiency

Subscript

B	Benzene
E	Ethylene
Eb	Ethylbenzene
H, hyd	Hydrogen
i	input
M	Methane
o	output
r	revers reaction
S, sty	Styrene
0	reactor 1 feed

LITERATURE CITED

1. Akpa, J.G. (2012). Simulation of an Isothermal Catalytic Membrane Reactor for the Dehydrogenation of Ethylbenzene, *Chem. Proc. Enginee. Res.* 3, 14–28, ISSN 2225–0913.

2. Arno Behr. (2017). Styrene production from ethyl benzene, Retrieved July 13, 2017 from (http://www.tc.bci.tu- dortmund.de/Downloads/Praktika/tc30_styrene_english.pdf.

3. Hermann, Ch., Quicker, E. & Dittmeyer, R. (1997). Mathematical simulation of catalytic dehydrogenation of ethylbenzene. *J. Memb. Sci.* 136, 161–172. DOI: 10.1016/S0376-7388(97)81990-4.

4. PRWeb, World Styrene Market Dynamics Reviewed. Retrieved July, 13, 2017, from http://www.prweb.com/releases/2012/9/prweb9930130.htm.

5. PRLog, Styrene Global Markets to 2020. Retrieved July, 13, 2017, from http://www.prlog.org/11727607-styrene-global-markets-to-2020-substitution-of-polystyrene-by-polypropylene.

6. Snyder, J.D. & Subramaniam, B. (1994). Novel Reverse Flow Strategy for Ethylbenzene Dehydrogenation in A Packed bed Reactor. *Chem. Enginee. Sci*. 49(24), 5565–5601. DOI: 10.1016/0009-2509(94)00287-8.

7. Haynes, T.N., Georgakis, C. & Caram, H.S. (1992). The Application of Reverse Flow Reactors to Endothermic Reactions. *Chem. Enginee. Sci.* 47(9–11), 2927–2932. DOI: 10.1016/0009-2509(92)87153-H.

8. Abdalla, B.K., Elnashaie, S.S.E.H., Alkhowaiter, S. & Elshishini, S.S. (1994). Intrinsic kinetics and industrial reactors modelling for the dehydrogenation of ethylbenzene to styrene on promoted iron oxide catalysts. *Appl. Catal. A: General* 113, 89–102. DOI: 10.1016/0926-860X(94)80243-2.

9. Hossain, M.M., Atanda, L., Al-Yassir, N., Al-Khattaf, S. (2012). Kinetics modeling of ethylbenzene dehydrogenation to styrene over a mesoporous alumina supported iron catalyst. *Chem. Enginee. J.* 207–208, 308–321. DOI: 10.1016/j.cej.2012.06.108.

10. Tamsilian, Y., Ebrahimi, A.N., Ramazani, S.A. & Abdollahzadeh, H. (2012). Modeling and sensitivity analysis of styrene monomer production process and investigation of catalyst behavior. *Comp. Chem. Enginee.* 40, 1–11. DOI: 10.1016/j.compchemeng.2012.01.014.

11. Zarubina, V. (2015). *Oxidative dehydrogenation of ethylbenzene under industrially relevant conditions: on the role of catalyst structure and texture on selectivity and stability*. PhD Thesis, University of Groningen, Netherland.

12. Lee, W.J. (2005). *Ethylbenzene Dehydrogenation into Styrene: Kinetic Modeling and Reactor Simulation*. PhD Thesis, Texas A&M.

13. Nederlof, C. (2012). *Catalytic dehydrogenations of ethylbenzene to styrene*. PhD thesis, University of Delft, Netherland.

14. Park, S.E. & Chang, J.S. (2004). Novel Process for Styrene from Ethylbenzene with Carbon Dioxide. 227th National Meeting of the American-Chemical Society, MAR 28-APR 01, 2004 (pp U1076-U1076), Anaheim, CA, USA. ISSN: 0065-7727.

15. Mimura, N. & Saito, M. (2000a). Dehydrogenation of ethylbenzene to styrene over Fe_2O_3/Al_2O_3 catalysts in the presence of carbon dioxide. *Catal. Today* 55, 173–178. DOI: 10.1016/S0920-5861(99)00236-9.

16. Mimura, N. & Saito, M. (200b). Dehydrogenation of ethylbenzene to styrene in the presence of CO_2. *Appl. Organometal. Chem.* 14, 773–777. DOI: 10.1002/1099-0739(200012)14

17. Cavani, F. & Trifiro, F. (1995). Alternative Processes for the Production of Styrene. *Appl. Catal. A*, 133, 219–239.DOI: 10.1016/0926-860X(95)00218-9.

18. Mimura, N., Takahara, I., Saito, M., Hattori, T., Ohkuma, K. & Ando, M. (1998). Dehydrogenation of ethylbenzene over iron oxide-based catalyst in the presence of carbon dioxide. *Catal. Today* 45, 60–64. DOI: 10.1016/S0920-5861(98)00246-6.

19. Abdalla, B.K., Elnashaie, S.S. E.H. (1994). Catalytic Dehydrogenation of Ethylbenzene to Styrene in Membrane Reactors. *AIChE* 40(12), 2055–2059. DOI: 10.1002/aic.690401215.

20. Vaezi, M.J., Babaluo, A.A. & Shafiei, S. (2015). Modeling of Ethylbenzene Dehydrogenation Membrane Reactor to Investigate the Potential Application of a Microporous Hydroxy Sodalite Membrane. *J. Chem. Petrol. Enginee.* 49(1), 51–62. ISSN: 2423–6721.

21. Gundersen, T. (2017). *Chapter 2.1 in Handbook of Process Integration Heat Integration -Targets and Heat Exchanger Network Design*, Retrieved July, 7, 2017. http://www.ivt.ntnu.no/ept/fag/tep4215/innhold/Handbook%20of%20PI%20- %20Chapter%202-1.pdf.

22. Yoon, S.G. Lee, J. & Park, S. (2007). Heat integration analysis for an industrial ethylbenzene plant using pinch analysis. *Appl. Ther. Enginee.* 27, 886–893. DOI: 10.1016/j.applthermaleng.2006.09.001.

23. Carra. S. & Fomi. L. (1965). Kinetics of Catalytic Dehydrogenation of Ethylbenzene to Styrene. *Engng. Chem. Proc. Des. Dev.* 4, 281–285. DOI: 10.1021/i260015a009.

24. Modell, D.J. (1972). *Optimization theory and applications: optimum temperature simulation of the styrene monomer reaction*. Chem. Enginee. Comput. Vol. 1. AIChE, New York.

25. Lee, W.J. & Froment, G.F. (2008). Ethylbenzene Dehydrogenation into Styrene: Kinetic Modeling and Reactor Simulation. *Ind. Eng. Chem. Res.* 47, 9183–9194. DOI: 10.1021/ie071098u.

26. James, D.H. & Castor, W.M. (1994). *Ullmann's encyclopedia of industrial chemistry*. Wiley. Vol. 25, 5th ed., p. 329.

27. Styrene Production, Retrieved July, 13, 2017. http://cbe.statler.wvu.edu/files/d/cd80e618-6d29-41a9-a854-275a995ed6cf/styrene12.pdf.

28. Hanyak, M.E. (2011). *Companion in Chemical Engineering: An Instructional Supplement*, CreateSpace Independent Publishing Platform, USA.

29. Smith, J.M., Van Ness, H.C. & Abbott, M.M. (2005). *Introduction to Chemical Engineering Thermodynamics*, 6th edition, McGraw Hills, USA.

30. Wall, G. (2011). Life Cycle Exergy Analysis of Renewable Energy System. *Renew. Energy J.* 4, 72–77. DOI: 10.2174/1876387101004010072.

31. Martinaitis, V., Streckiene, G., Biekša, D. & Bielskus, J. (2016). The exergy efficiency assessment of heat recovery exchanger for air handling units, using a state property – Coenthalpy. *Appl. Therm. Enginee.* 108, 388–397. DOI: 10.1016/j.applthermaleng.2016.07.118.

32. Shenoy, U.V. (1995). *Heat Exchange Network Synthesis: Process Optimization by Energy and Resource Analysis*. Gulf Publ. Co., Houston, TX.

33. Linnhoff, B. (1993). Pinch analysis- A state of the art overview. *Trans. Inst. Chem. Eng. Chem. Eng. Res. Des*. 71, Part A5, 503–522. ISSN: 0263-8762.

34. Gundersen, T. & Naess, L. (1988). The synthesis of cost optimal heat exchanger networks: An industrial review of the state of the art. *Comput. Chem. Enginee.* 12(6), 503–530. DOI: 10.1016/0890-4332(90)90084-W.

35. Douglas, J.M. (1988). *Conceptual Design of Chemical Processes*, McGraw Hill, New York.

36. El-Halwagi, M.M. (2012). *Sustainable Design Through Process Integration*, 1st Ed., Butterworth-Heinemann, USA.

37. Klemes, J. (2013). *Handbook of Process Integration* (PI), Woodhead Publishing, USA.